Data repository items for

"Nanocrystalline slip zones in calcite fault gouge show intense CPO: Crystal plasticity at sub-seismic slip rates at 18-150°C"

Berend A. Verberne*, Johannes H. P. de Bresser, André R. Niemeijer, Christopher J. Spiers, D. A. Matthijs de Winter and Oliver Plümper

**Corresponding author email: B.A.Verberne@uu.nl*

This file contains supplementary text, data, and figures, ordered into 6 Data Repository items:

Data Repository item DR1: **Simulated gouge grain size distributions**

Data Repository item DR2: **Experimental methodology and Procedures**

Data Repository item DR3: **Electron microscopy methods**

Data Repository item DR4: **Frictional strength vs. Shear displacement data**

Data Repository item DR5: **Photomosaics of samples $CaCO_3$-RT-dry, $CaCO_3$-100-dry & $CaCO_3$-150-dry.**

Data Repository item DR6: **Background on the microstructures of Fig. 4**

Data Repository tem DR1

SIMULATED GOUGE GRAIN SIZE DISTRIBUTIONS

FIGURE DR1. Initial grain size distributions of simulated Xujiahe limestone and $CaCO_3$ gouge used in our experiments. Measured using a laser particle sizer.

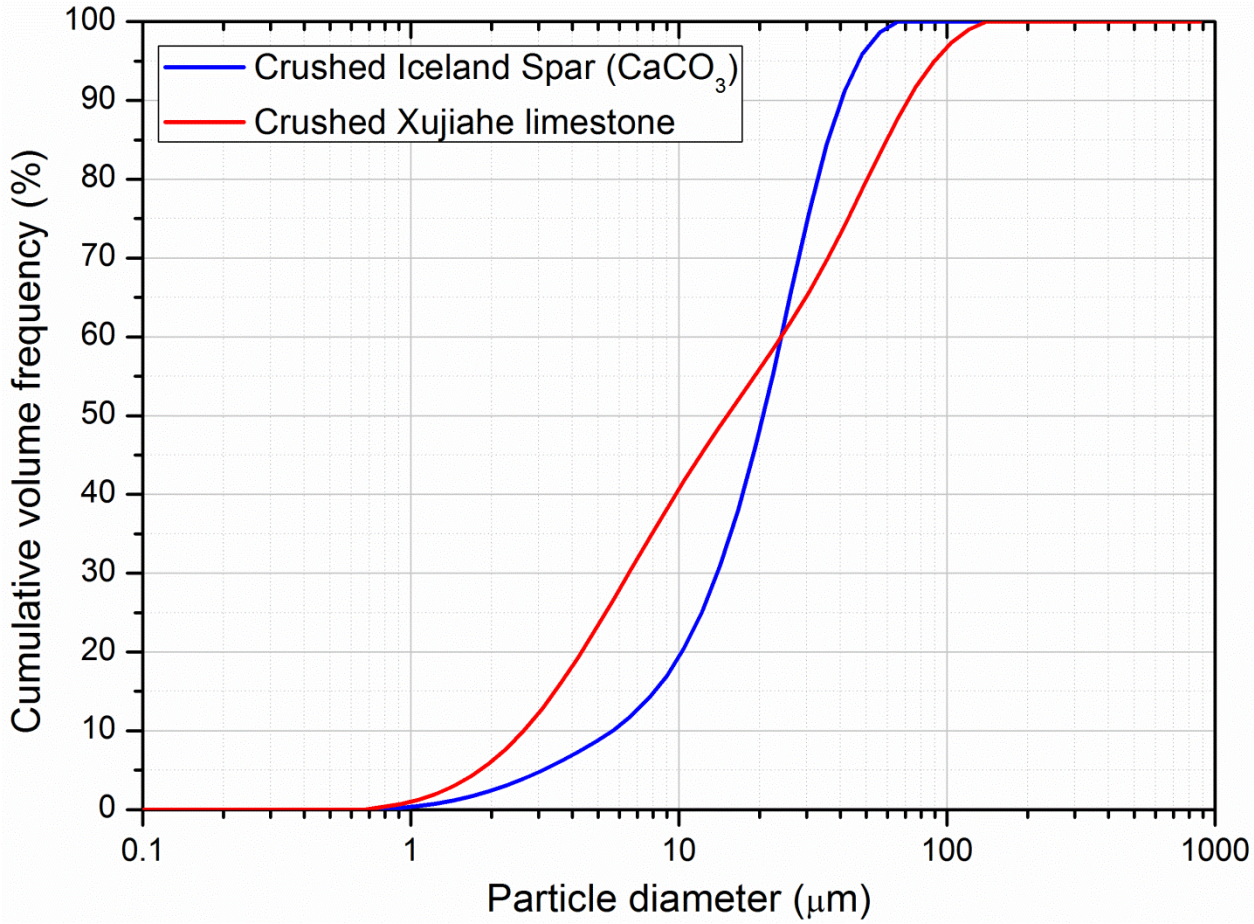

Data Repository Item DR2

EXPERIMENTAL METHODOLOGY AND PROCEDURES

The experimental apparatus used consisted of a triaxial deformation apparatus in a yoke assembly (Fig. DR2A), comprising a self-compensated-volume silicon-oil confining medium pressure vessel plus an electro-servo-controlled ram for axial loading. Axial force, hence shear stress (τ) acting on the sample layer, was measured using an internal force gauge with a resolution of ~0.02 MPa (Fig. DR2A). Displacement was measured externally with a Linear Variable Differential Transformer (LVDT), and corrected for apparatus distortion using calibrations performed with a steel dummy. Temperature was measured using a K-type thermocouple located within 5 mm of the sample (Fig. DR2B). Individual direct shear piston dimensions are 35 mm in diameter by 70 mm in total length, comprising a 35x49 mm grooved sample-piston interface, a 35x9 mm smooth surface, plus a cylindrical 35x12 mm end-piece (Fig. DR2B). The sample-piston interface consisted of a set of 0.1 mm regular spaced triangular grooves, 0.1 mm wide and 0.05 mm deep (Fig. DR2C).

In preparing each experiment, all loose gouge samples were mixed into a paste using demineralized water, in proportions of roughly 4:1 gouge to water. A purpose-built jig allowed for easy emplacement of a ~1.1 mm thick gouge paste layer onto the sample-piston interface, forming a plate measuring 35 mm wide by 47 mm long. The sample was dried in an oven at 115˚C for at least 4 hours. We confirmed complete dehydration of the sample by using a dummy sample-paste, and weighing before and after drying. In order to avoid contamination from atmospheric water vapor, the sample assembly was sealed while the piston plus sample layer were still hot. All experiments used two Indium bars (cuboids) measuring 35x1x1 mm at each end of the sample layer to avoid 1) volume-loss of the initial gouge layer, 2) introduction of

silicone putty into the sample, and 3) wedging of PTFE (Poly-Tetra-Fluoro-Ethylene, a.k.a. teflon) foil between the sample and the direct shear piston interface. After positioning the indium bars, a half-cylinder steel spacer is laid onto the remaining smooth surface, and the second direct shear piston is emplaced, i.e. with the grooved surface corresponding to the sample layer. Subsequently, another half-cylinder steel spacer is inserted into the remaining void and the assembly is positioned vertically. To allow for easier handling we rigidified the thus prepared assembly using a jacket of heat-shrink Fluorinated Ethylene Propylene (FEP) tubing of ~0.4 mm initial thickness. The heat-shrunk FEP is cut with a razor, preserving only the portion covering the sample layer, so that the steel spacers can be removed from the voids. After cleaning with a moist swab, the voids are plugged with a weak displacement accommodating filler, constructed chronologically using 1) a ~7x10 cm sheet of 0.05 mm thick PTFE film, 2) a specially designed L-shaped EPDM (Ethylene Propylene Diene Monomer) rubber piece of 1 mm thickness with a 35 mm diameter half-cylindrical base, 3) another sheet (~7x10 cm) of 0.05 mm thick PTFE film, 4) ~3.8 g of classic white silicone putty and, finally, 5) a wrapping of PTFE thread seal tape to hold the silicone putty in place. The PTFE foil plus L-shaped EPDM rubber piece is used to ensure isolation of the sample layer from the silicone putty, which flows outwards upon closure of the voids, i.e. upon axial loading of the sample assembly. The entire assembly, including sample layer, FEP and the displacement-accommodating void-fill are jacketed with an EPDM rubber sleeve, and mounted between two forcing blocks plus an Aluminum spacer for reducing oil-convection during experiments at high temperatures (Fig. DR2A).

For each experiment, the velocity dependence of friction was quantified using the rate parameter $(a-b) \approx \Delta\mu_{ss}/\Delta \ln v$. This was done using the change in steady-state strength ($\Delta\mu_{ss}$), or, in the case of stick-slip, the change in maximum strength, obtained per velocity step (Δv). In doing

this, all data were corrected for background slip hardening or softening by linear detrending (following e.g. *Blanpied et al., 1995*).

To examine potential effects of the sample assembly to the measurement of gouge layer frictional properties we performed test runs at room temperature (~18°C), at a normal stress σ_n = 50 MPa, using 35x47x1 mm sheets of PTFE and Indium. The peak shear strength measured in these tests was ≤3 MPa and ≤4 MPa for the PTFE and Indium sheets respectively (Fig. DR3). This suggests that the sample assembly has a very low contribution to the total frictional strength measured, i.e. <<4 MPa. In response to velocity steps we invariably found velocity strengthening behavior, for both PTFE and Indium. To investigate sample-assembly effects to the friction rate parameter (a-b), we performed a test on talc gouge at room temperature and σ_n = 50 MPa for comparison with previously published data. The results showed a peak coefficient of sliding friction (μ) of 0.18, decreasing to a residual value of 0.14-0.16 (Fig. DR3). In response to velocity steps the talc gouge showed velocity strengthening behavior, with a value of (a-b) = $\Delta\mu_{ss}/\Delta\ln(v)$ of 0.0061 ± 0.0005, averaged over the five velocity steps applied. These data are in good agreement with data from triaxial saw-cut experiments on talc gouge reported previously (*Moore & Lockner, 2008*). Therefore we are confident that the sample assembly used in this study has a negligible effect to the frictional properties measured from our sample layers.

Experimental procedure

In performing each experiment, the sample assembly including the gouge layer was loaded into the pressure vessel and allowed to equilibrate under the desired test temperature and pressure. The silicone-oil temperature increases rapidly in the first minute after heating, followed by stabilization to a value near the furnace setpoint temperature. Consequently, in the first minute after switching on the internal furnace, the confining pressure increased at a rate of ~1-2 MPa/s,

followed by slow approach to a near-constant value. Confining pressure was applied using a diaphragm pump, and held below the desired normal stress through intermittent bleeding of the pressure vessel. During a test, confining pressure was held constant to within ~0.1 MPa using a 20 ml hand pump. Equilibration of the testing apparatus took from around 1 hour at room temperature to >4 hours at 150˚C.

Once the system was at steady-state we used a ramp generator connected to a digital interface to apply a desired displacement rate. The initial displacement rate used in each experiment was 1 μm/s. After achieving steady-state sliding, or stick-slip at a constant peak stress, the displacement rate was stepped to 0.1, 10, 1, 0.1, 10, and 1 μm/s, employing 0.2-1.0 mm displacement intervals. In terminating each experiment, the axial loading ram is backed off at a rate 10 μm/s. For experiments at a temperature higher than room temperature, the assembly was cooled using an internal water cooling system (Fig. DR2A), and depressurized slowly (< ~0.5 MPa/s) to atmospheric conditions. After removing from the pressure vessel and dismantling the assembly, the sheared gouge layer was recovered from the sample-piston interface using duct-tape before impregnation using Araldite 2020 epoxy resin.

REFERENCES CITED

Blanpied, M. L., Lockner, D. A., and Byerlee, J. D., 1995, Frictional slip of granite at hydrothermal conditions: Journal of Geophysical Research, v. 100, no. B7, p. 13045-13064

Moore, D.E., and Lockner, D.A., 2008, Talc friction in the temperature range 25°-400°C: Relevance for Fault-Zone Weakening: Tectonophysics, v. 449, no. 1-4, p. 120-132.

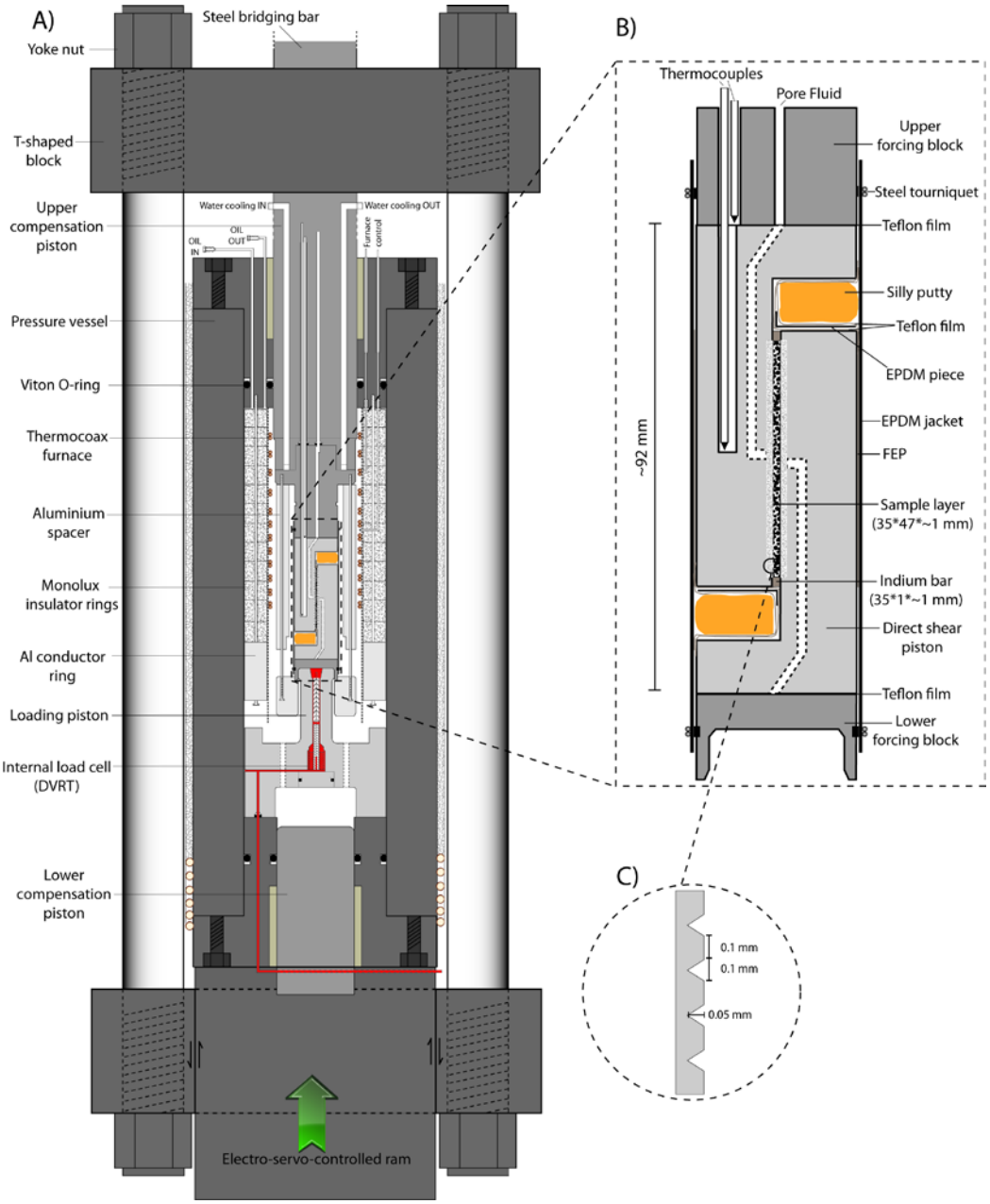

FIGURE DR2. Schematic cross-sections of the apparatus used plus sample assembly. A). Self-compensating volume, silicone-oil confining medium pressure vessel. B). Direct shear sample assembly. C). Groove pattern of the piston set used.

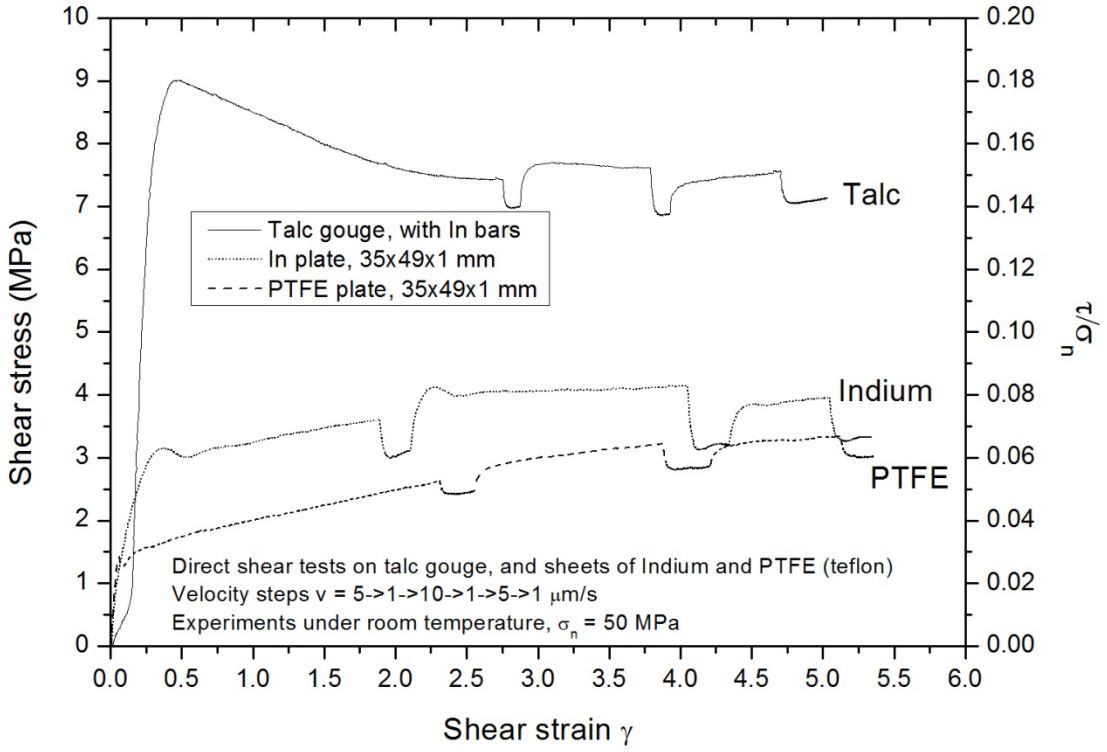

FIGURE DR3. Plots of frictional strength against shear strain showing data from direct shear tests on 35x49x1 mm sheets of PTFE and Indium, and a 35x47x1 mm Talc gouge layer.

Data Repository Item DR3

ELECTRON MICROSCOPY METHODS

We used a Nova Nanolab 600 FIB-SEM (focused ion beam – scanning electron microscope), installed at the Department of Biology of Utrecht University, for detailed analysis of the shear band microstructures (Fig. 4A,B, DR6). FIB-SEM combines the milling capabilities of the ion beam and the imaging capabilities of the electron beam. Momentum-transfer from Gallium ions to the sample causes local sputtering, enabling sectioning at micron-scales with nano-scale precision, and the excavation of electron transparent foils used for further analysis, e.g. using transmission electron microscopy (TEM) *(e.g. Volkert & Minor, 2007)*. Optical imaging in the SEM is done in secondary electron (SE) mode (DR6 - top row, center image). Cross sections and FIB-SEM tomography series are imaged in backscatter electron (BSE) mode. TEM foils were prepared using FIB-SEM following standard protocol *(e.g. Mayer et al., 2007)*, i.e. a selected boundary shear cross-section was trenched using the FIB-SEM, extracted using a micromanipulator, and then mounted on a C-mount TEM grid. The section was polished to a thickness ~100 nm, yielding an electron transparent TEM foil. For some foils used in this study (e.g. those used for Fig. 4C, E), an additional polishing step was performed to locally reduce the thickness of the foil to ~50 nm.

To investigate the crystallographic orientation distribution of calcite grains in the shear band, we explored transmission-electron backscattered diffraction (t-EBSD) *(Keller & Geiss, 2011; Trimby et al., 2012)*. 'Standard' EBSD was discounted because of the extremely small grain size and the grain size heterogeneity in the shear band core. In conducting t-EBSD, we attached the C-mount grid with a ~50 nm thick foil to a pre-tilted holder, obtaining an angle of approximately 20° relative to the horizontal. Forward diffracted electrons were captured using a

Nordlys II EBSD detector mounted on the FIB-SEM, at an acceleration voltage of 30 kV. All Kikuchi band diffraction patterns were indexed manually. Despite obtaining some promising diffraction data just ~15% out of >5000 spot analyses yielded a diffraction pattern strong enough for indexation, which were demonstrably from the larger grains in the shear band. Thus, our t-EBSD analyses did not allow for a statistically robust data set.

TEM observations on electron transparent foils were performed in a Technai 20F TEM equipped with a field-emission gun and operated at 200 kV. Characterization of the nanograins within the shear bands was performed using high-resolution (HR-) TEM imaging (Fig. 4D). In addition, systematic bright- (Fig. 4C) and dark-field diffraction (Fig. 4E) contrast imaging was used to investigate the crystallographic preferred orientation of nanograins within the shear band cores. It is to note that due to camera resolution and differences in magnification the apparent illumination of nanograins within the shear band core is influenced, i.e. higher magnification images (more pixels per unit area) result in a more effective capture of illuminated grains of a certain size (compare Fig. DR4 and Fig. 4E).

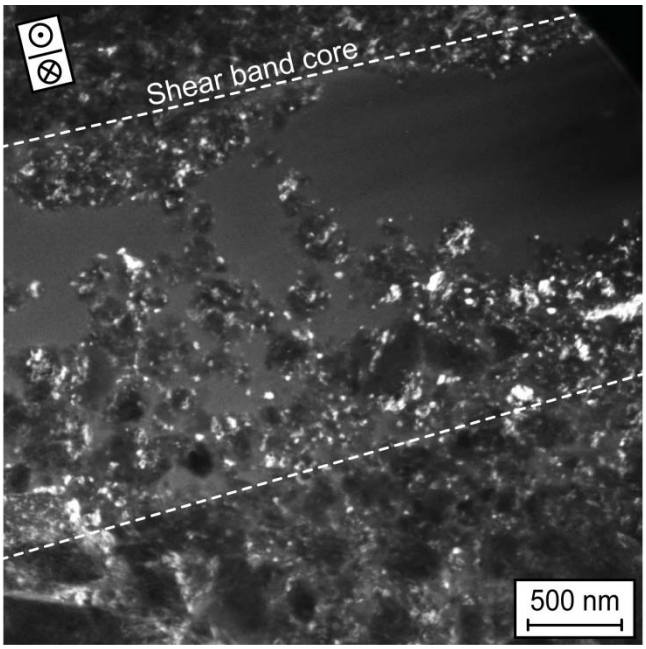

FIGURE DR4. Higher resolution dark field image, highlighting the preferred nanograin illumination within the shear band core.

REFERENCES CITED

Keller, R. R., and Geiss, R. H., 2011, Transmission EBSD from 10 nm domains in a scanning electron microscope: Journal of Microscopy, doi:10.1111/j.1365-2818.2011.03566.x

Mayer, J., Gianuzzi, L. A., Kamino, T. & Michael, J. 2007. TEM sample preparation and FIB-induced damage. *MRS Bulletin*, **32**, 5, 400-407, doi:10.1557/mrs2007.63.

Trimby, P.W., 2012. Orientation mapping of nanostructured materials using transmission Kikuchi diffraction in the scanning electron microscope. Ultramicroscopy. 2012 Sep; 120:16-24. doi: 10.1016/j.ultramic.2012.06.004. Epub 2012 Jun 15.

Volkert, C. A. & Minor, A. M, 2007, Focused ion beam microscopy and micromachining: MRS Bulletin, v. 32, no. 5, p. 389-395.

Data Repository Item DR4

FRICTIONAL STRENGTH VS. SHEAR DISPLACEMENT DATA

FIGURE DR5. Apparent coefficient of friction μ against shear displacement curves for dry direct shear experiments on simulated gouges of Xujiahe limestone (red) and $CaCO_3$ Iceland Spar (blue), at a normal stress of ~50 MPa, at temperatures ranging from room temperature (~18°C) to ~150°C. For all experiments the initial shear displacement rate is 1 μm/s, which is stepped following the scheme indicated between vertical bars.

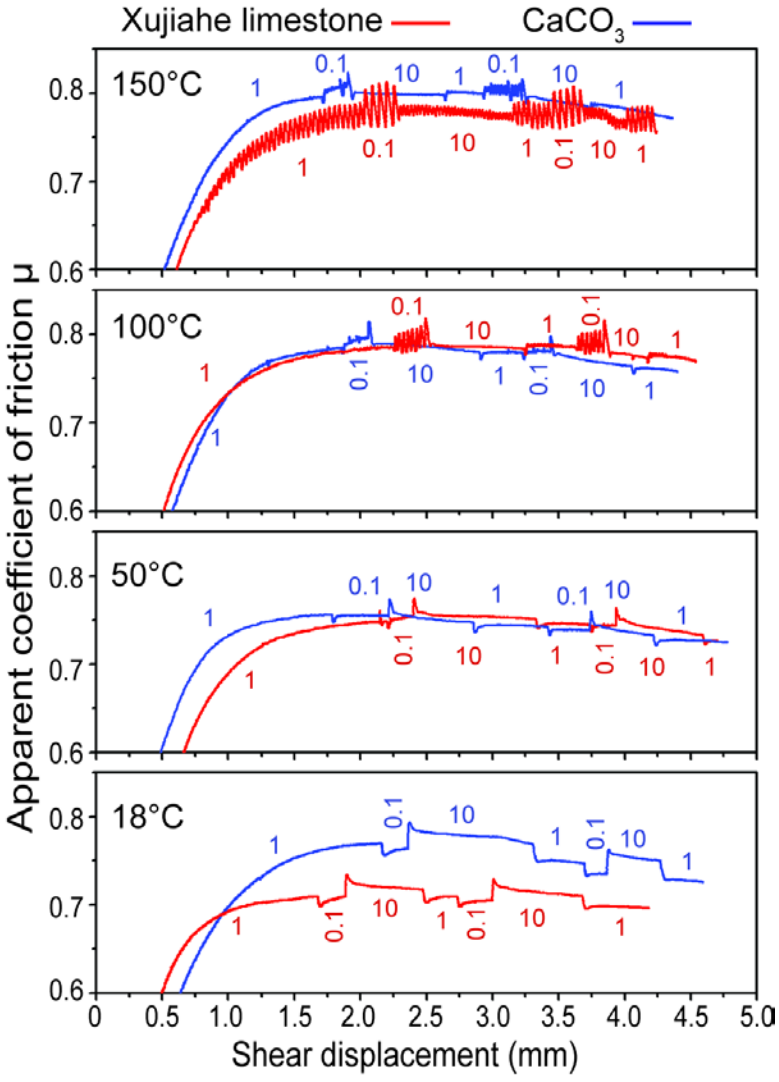

Data Repository Item 5: Photomosaics of thin sections

$CaCO_3$, RT, dry
In XPL, with gypsum plate

1 mm

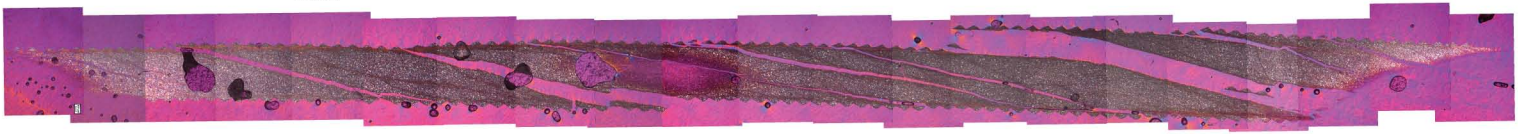

Total # of R_1 shears: 16
Length section: 26.9 mm
$\rho(R_1)$: 0.61 mm^{-1}

Angle of R_1 shear in centre of layer to the shear plane ranges ~5-24°

$CaCO_3$, 100°C, dry
In XPL, with gypsum plate

1 mm

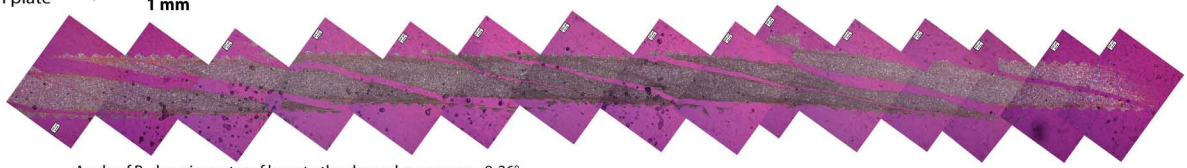

Total # of R_1 shears: 13
Length section: 21.5 mm
$\rho(R_1)$: 0.60 mm^{-1}

Angle of R_1 shear in centre of layer to the shear plane ranges ~8-26°

$CaCO_3$, 150°C, dry
In XPL, with gypsum plate

1 mm

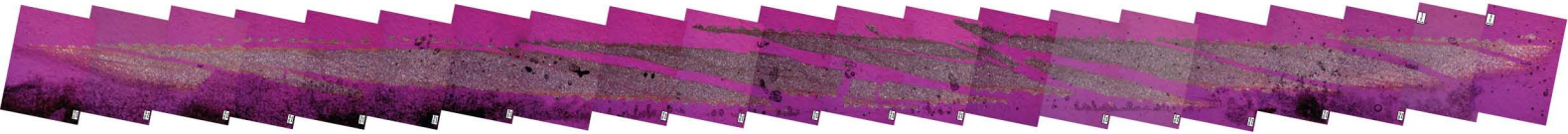

Total # of R_1 shears: 15
Length section: 27 mm
$\rho(R_1)$: 0.56 mm^{-1}

Angle of R_1 shear in centre of layer to the shear plane ranges ~6-20°

Item DR6. Background on the microstructures presented in Figure 4

Figure 4A, C-E:

*The cross-section of Fig. 4A was obtained similarly, but then from sample $CaCO_3$-RT-dry.

Sample $CaCO_3$-150-dry *

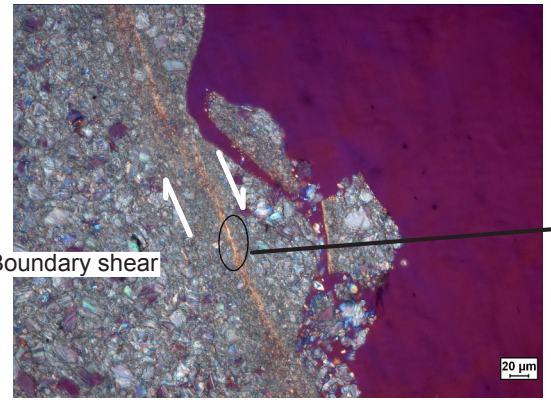

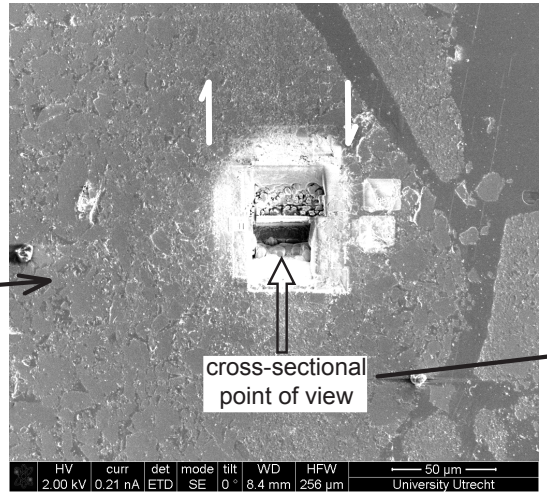

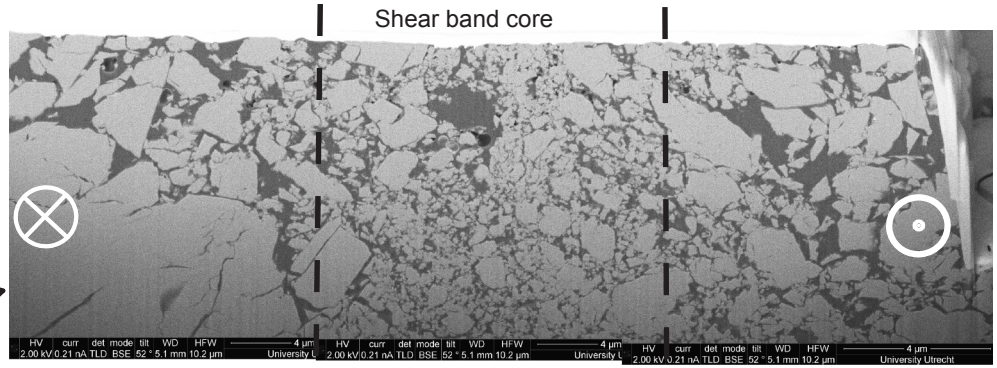

The TEM foil used for Figs. 4C-E was prepared from an analogous cross section, from **this** FIB-milled trench.

Figure 4B:

Fig. 4B was obtained from an analogous cross section in a Slice & View series from **this** FIB-milled trench.

Sample $CaCO_3$-150-dry

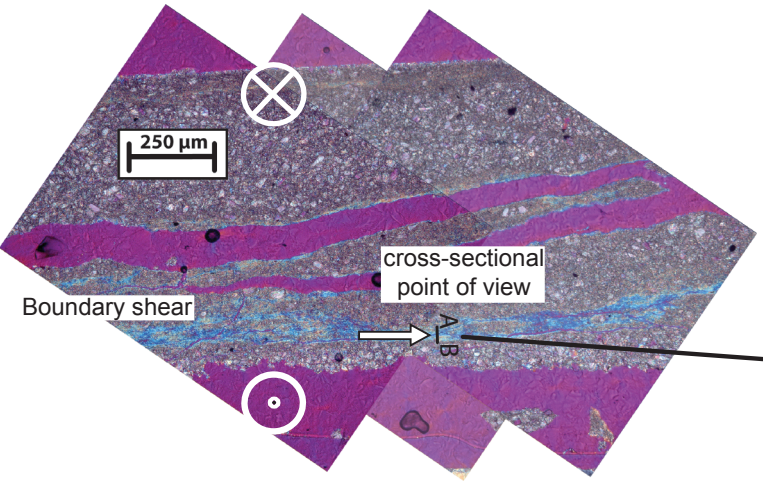

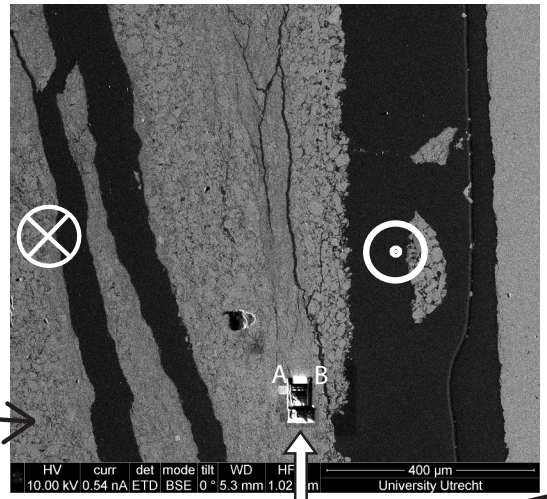

BSE image from Slice-and-view series